

Reducing dopant variability in nano-devices

Jesse Maassen^{*†} and Hong Guo^{*}

^{*}Department of Physics, McGill University, Montreal, Quebec, Canada H3A 2T8

[†]Network for Computational Nanotechnology, Purdue University, West Lafayette, Indiana 47907, USA
e-mail: maassenj@physics.mcgill.ca

Random dopant fluctuations (RDF) [1], due to changes in the particular microscopic arrangement of dopant atoms from one device to another, is a concerning source of variability. In this work, we demonstrate by means of first principles transport simulations how eliminating dopants from certain regions in a Si channel can suppress leakage currents and greatly reduce device variations.

The goal is to study how the location of dopant atoms affects OFF-state leakage current. This is done by confining the B or P dopants to 1.1 nm regions along the Si channel (see Fig. 1), in which the dopants are randomly distributed. We consider n-p-n and p-n-p device structures with channel lengths L ranging from 6.5 nm to 15.2 nm. The source/drain are uniformly doped to $5 \times 10^{19} \text{ cm}^{-3}$ and the channel doping is fixed to $5 \times 10^{18} \text{ cm}^{-3}$. The device is modeled using *ab initio* quantum transport theory, combining density functional theory with nonequilibrium Green's functions, as implemented in the NANODSIM simulation package [3]. This particular method uniquely handles random atomic disorder [2], such as doping. Lastly, we predict the experimental Si band gap of 1.1 eV using the modified Becke-Johnson exchange potential [4].

Fig. 2 shows the tunneling conductance G as a function of doping location for both B- and P-doped channels of length $L = 10.9 \text{ nm}$, at $T = 0$ and $V = 0$. Large conductance variations are observed ($G_{\text{MAX}}/G_{\text{MIN}} \approx 50$) with center-channel doping leading to the smallest G . The relative conductance around the case of uniform doping G_{UNI} is shown in Fig. 3. The largest deviations occur in the vicinity of the electrodes. The source of the variations in leakage current is the change in potential profile induced by the dopants, as shown in Fig. 4. Fig. 5 shows the WKB conductance calculated from the potential profile in Fig. 4. The fit is good, indicating that the conductance depends solely on barrier shape.

In fact, the integrated potential profile affects the tunneling probability exponentially, which explains the dramatic changes in G .

In Fig. 6, we show how varying L affects leakage current. Two trends are clear: (i) the tunneling current decreases significantly with L , which is a well-known short-channel effect and (ii) the variations in G increase dramatically with L . The latter is highlighted in Fig. 7, where G_{MAX} and G_{MIN} are plotted versus L in addition to the ratio of $G_{\text{MAX}}/G_{\text{MIN}}$. For $L = 6.5 \text{ nm}$ the G ratio is ≈ 2 , while for $L = 15.2 \text{ nm}$ one finds a value approaching 10^5 . Thus, the effect of doping location is very strongly L -dependent, and appears to be very important in the case of $L = 15.2 \text{ nm}$. An important point is that one can significantly reduce leakage current and device variations by avoiding doping near the source/drain. Fig. 8 shows the distance from the leads at which the doping layer yields a G less than that of uniform doping. A linear fit shows that this distance is roughly 20% of L . Up to now, we only considered tunneling in the zero-temperature limit, by calculating the leakage current at $T = 300 \text{ K}$ we determine that the G variations are enhanced $2\times$ (for $L = 10.9 \text{ nm}$) due to thermally excited carriers.

The authors acknowledge support from NSERC, FQRNT and CIFAR.

REFERENCES

- [1] A. Asenov, A. R. Brown, J. H. Davies, S. Kaya, and G. Slavcheva, *Simulation of intrinsic parameter fluctuations in decanometer and nanometer-scale MOSFETs*, IEEE Trans. Electron Devices **50**, 1837 (2003).
- [2] Y. Ke, K. Xia, and H. Guo, *Disorder Scattering in Magnetic Tunnel Junctions: Theory of Nonequilibrium Vertex Correction*, Phys. Rev. Lett. **100**, 166805 (2008).
- [3] Nanoacademic Technologies, <http://nanoacademic.ca/>.
- [4] F. Tran and P. Blaha, *Accurate Band Gaps of Semiconductors and Insulators with a Semilocal Exchange-Correlation Potential*, Phys. Rev. Lett. **102**, 226401 (2009).

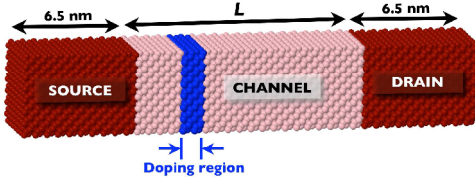


Fig. 1. Diagram of the simulated system. The doping length is set to 1.1 nm with a doping concentration of $5 \times 10^{18} \text{ cm}^{-3}$. Source/drain leads are uniformly doped to $5 \times 10^{19} \text{ cm}^{-3}$. Periodic boundary conditions are applied in the plane perpendicular to transport.

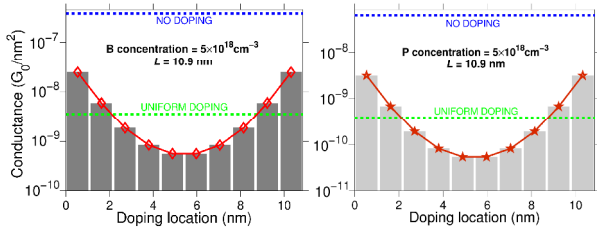


Fig. 2. Tunneling conductance G versus doping location for B- and P-doped channels with $L = 10.9 \text{ nm}$. Blue and green lines correspond to G with no doping and uniform doping, respectively.

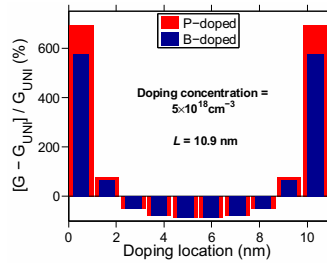


Fig. 3. Relative conductance variation around the case of uniform doping versus doping location.

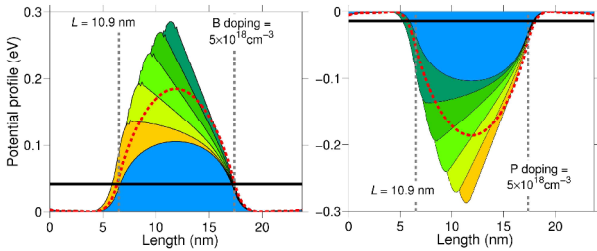


Fig. 4. Potential profile at each point along the simulation box. From front to back the dopants are located in layers starting next to the source and ending in the center of the channel. Blue area curve: no doping. Red dashed curve: uniform doping. Solid black line: Fermi level.

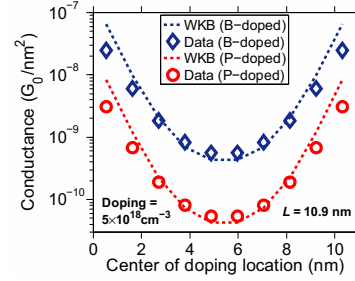


Fig. 5. Simulated and WKB (from the potential in Fig. 4) tunneling conductance. We use $m_e^* = 0.26$, $m_h^* = 0.36$.

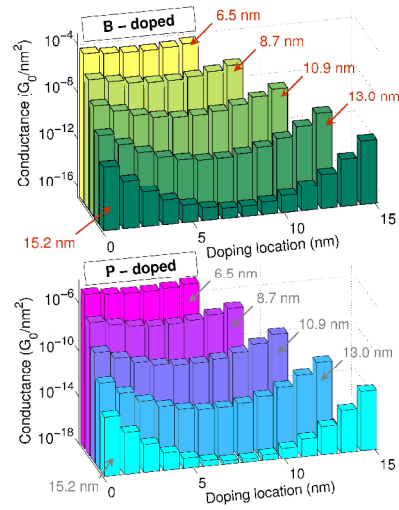


Fig. 6. G versus doping location as a function of L .

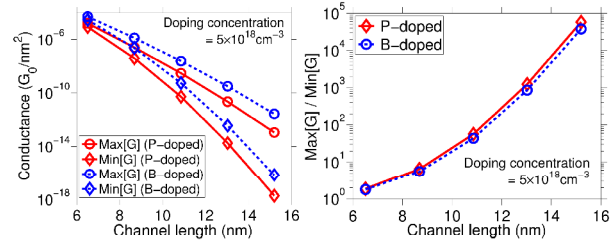


Fig. 7. Maximum and minimum G (from Fig. 6) and ratio $G_{\text{MAX}}/G_{\text{MIN}}$ versus channel length L .

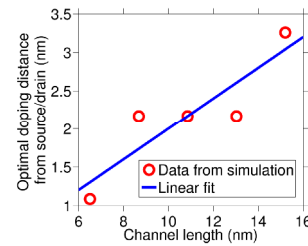


Fig. 8. Distance from the leads to avoid doping such that G is less than that of uniform doping.